

## Initial performance of the CUORE detector

J. S. Cushman<sup>1</sup>, C. Alduino<sup>2</sup>, K. Alfonso<sup>3</sup>, F. T. Avignone III<sup>2</sup>,  
 O. Azzolini<sup>4</sup>, G. Bari<sup>5</sup>, F. Bellini<sup>6,7</sup>, G. Benato<sup>8</sup>, A. Bersani<sup>9</sup>,  
 M. Biassoni<sup>10,11</sup>, A. Branca<sup>12,13</sup>, C. Brofferio<sup>10,11</sup>, C. Bucci<sup>14</sup>,  
 A. Camacho<sup>4</sup>, A. Caminata<sup>9</sup>, L. Canonica<sup>15,14</sup>, X. G. Cao<sup>16</sup>,  
 S. Capelli<sup>10,11</sup>, L. Cappelli<sup>14</sup>, L. Cardani<sup>7</sup>, P. Carniti<sup>10,11</sup>, N. Casali<sup>7</sup>,  
 L. Cassina<sup>10,11</sup>, D. Chiesa<sup>10,11</sup>, N. Chott<sup>2</sup>, M. Clemenza<sup>10,11</sup>,  
 S. Copello<sup>17,9</sup>, C. Cosmelli<sup>6,7</sup>, O. Cremonesi<sup>11</sup>, R. J. Creswick<sup>2</sup>,  
 A. D'Addabbo<sup>14</sup>, D. D'Aguanno<sup>14,18</sup>, I. Dafinei<sup>7</sup>, C. J. Davis<sup>1</sup>,  
 S. Dell'Oro<sup>19,14,20</sup>, M. M. Deninno<sup>5</sup>, S. Di Domizio<sup>17,9</sup>,  
 M. L. Di Vacri<sup>14,21</sup>, A. Drobizhev<sup>8,22</sup>, D. Q. Fang<sup>16</sup>, M. Faverzani<sup>10,11</sup>,  
 E. Ferri<sup>11</sup>, F. Ferroni<sup>6,7</sup>, E. Fiorini<sup>11,10</sup>, M. A. Franceschi<sup>23</sup>,  
 S. J. Freedman<sup>22,7,a</sup>, B. K. Fujikawa<sup>22</sup>, A. Giachero<sup>11</sup>, L. Gironi<sup>10,11</sup>,  
 A. Giuliani<sup>24</sup>, L. Gladstone<sup>15</sup>, P. Gorla<sup>14</sup>, C. Gotti<sup>10,11</sup>,  
 T. D. Gutierrez<sup>25</sup>, K. Han<sup>26</sup>, K. M. Heeger<sup>1</sup>,  
 R. Hennings-Yeomans<sup>8,22</sup>, H. Z. Huang<sup>3</sup>, G. Keppel<sup>4</sup>,  
 Yu. G. Kolomensky<sup>8,22</sup>, A. Leder<sup>15</sup>, C. Ligi<sup>23</sup>, K. E. Lim<sup>1</sup>, Y. G. Ma<sup>16</sup>,  
 L. Marini<sup>17,9</sup>, M. Martinez<sup>6,7,27</sup>, R. H. Maruyama<sup>1</sup>, Y. Mei<sup>22</sup>,  
 N. Moggi<sup>28,5</sup>, S. Morganti<sup>7</sup>, S. S. Nagorny<sup>14,20</sup>, T. Napolitano<sup>23</sup>,  
 M. Nastasi<sup>10,11</sup>, C. Nones<sup>29</sup>, E. B. Norman<sup>30,31</sup>, V. Novati<sup>24</sup>,  
 A. Nucciotti<sup>10,11</sup>, I. Nutini<sup>14,20</sup>, T. O'Donnell<sup>19</sup>, J. L. Ouellet<sup>15</sup>,  
 C. E. Pagliarone<sup>14,18</sup>, M. Pallavicini<sup>17,9</sup>, V. Palmieri<sup>4</sup>, L. Pattavina<sup>14</sup>,  
 M. Pavan<sup>10,11</sup>, G. Pessina<sup>11</sup>, C. Pira<sup>4</sup>, S. Pirro<sup>14</sup>, S. Pozzi<sup>10,11</sup>,  
 E. Previtali<sup>11</sup>, F. Reindl<sup>7</sup>, C. Rosenfeld<sup>2</sup>, C. Rusconi<sup>2,14</sup>, M. Sakai<sup>3</sup>,  
 S. Sangiorgio<sup>30</sup>, D. Santone<sup>14,21</sup>, B. Schmidt<sup>22</sup>, J. Schmidt<sup>3</sup>,  
 N. D. Scielzo<sup>30</sup>, V. Singh<sup>8</sup>, M. Sisti<sup>10,11</sup>, L. Taffarello<sup>12</sup>,  
 F. Terranova<sup>10,11</sup>, C. Tomei<sup>7</sup>, M. Vignati<sup>7</sup>, S. L. Wagaarachchi<sup>8,22</sup>,  
 B. S. Wang<sup>30,31</sup>, H. W. Wang<sup>16</sup>, B. Welliver<sup>22</sup>, J. Wilson<sup>2</sup>, K. Wilson<sup>2</sup>,  
 L. A. Winslow<sup>15</sup>, T. Wise<sup>1,32</sup>, L. Zanotti<sup>10,11</sup>, G. Q. Zhang<sup>16</sup>,  
 S. Zimmermann<sup>33</sup>, and S. Zucchelli<sup>28,5</sup>

<sup>1</sup> Wright Laboratory, Department of Physics, Yale University, New Haven, CT 06520, USA

<sup>2</sup> Department of Physics and Astronomy, University of South Carolina, Columbia, SC 29208, USA

<sup>3</sup> Department of Physics and Astronomy, University of California, Los Angeles, CA 90095, USA

<sup>4</sup> INFN – Laboratori Nazionali di Legnaro, Legnaro (Padova) I-35020, Italy

<sup>5</sup> INFN – Sezione di Bologna, Bologna I-40127, Italy

<sup>6</sup> Dipartimento di Fisica, Sapienza Università di Roma, Roma I-00185, Italy

<sup>7</sup> INFN – Sezione di Roma, Roma I-00185, Italy

<sup>8</sup> Department of Physics, University of California, Berkeley, CA 94720, USA

<sup>9</sup> INFN – Sezione di Genova, Genova I-16146, Italy

<sup>10</sup> Dipartimento di Fisica, Università di Milano-Bicocca, Milano I-20126, Italy

<sup>11</sup> INFN – Sezione di Milano Bicocca, Milano I-20126, Italy

<sup>12</sup> INFN – Sezione di Padova, Padova I-35131, Italy<sup>13</sup> Dipartimento di Fisica e Astronomia, Università di Padova, I-35131 Padova, Italy<sup>14</sup> INFN – Laboratori Nazionali del Gran Sasso, Assergi (L’Aquila) I-67100, Italy<sup>15</sup> Massachusetts Institute of Technology, Cambridge, MA 02139, USA<sup>16</sup> Shanghai Institute of Applied Physics, Chinese Academy of Sciences, Shanghai 201800, China<sup>17</sup> Dipartimento di Fisica, Università di Genova, Genova I-16146, Italy<sup>18</sup> Dipartimento di Ingegneria Civile e Meccanica, Università degli Studi di Cassino e del Lazio Meridionale, Cassino I-03043, Italy<sup>19</sup> Center for Neutrino Physics, Virginia Polytechnic Institute and State University, Blacksburg, Virginia 24061, USA<sup>20</sup> INFN – Gran Sasso Science Institute, L’Aquila I-67100, Italy<sup>21</sup> Dipartimento di Scienze Fisiche e Chimiche, Università dell’Aquila, L’Aquila I-67100, Italy<sup>22</sup> Nuclear Science Division, Lawrence Berkeley National Laboratory, Berkeley, CA 94720, USA<sup>23</sup> INFN – Laboratori Nazionali di Frascati, Frascati (Roma) I-00044, Italy<sup>24</sup> CSNSM, Univ. Paris-Sud, CNRS/IN2P3, Universit Paris-Saclay, 91405 Orsay, France<sup>25</sup> Physics Department, California Polytechnic State University, San Luis Obispo, CA 93407, USA<sup>26</sup> INPAC and School of Physics and Astronomy, Shanghai Jiao Tong University; Shanghai Laboratory for Particle Physics and Cosmology, Shanghai 200240, China<sup>27</sup> Laboratorio de Fisica Nuclear y Astroparticulas, Universidad de Zaragoza, Zaragoza 50009, Spain<sup>28</sup> Dipartimento di Fisica e Astronomia, Alma Mater Studiorum – Università di Bologna, Bologna I-40127, Italy<sup>29</sup> Service de Physique des Particules, CEA / Saclay, 91191 Gif-sur-Yvette, France<sup>30</sup> Lawrence Livermore National Laboratory, Livermore, CA 94550, USA<sup>31</sup> Department of Nuclear Engineering, University of California, Berkeley, CA 94720, USA<sup>32</sup> Department of Physics, University of Wisconsin, Madison, WI 53706, USA<sup>33</sup> Engineering Division, Lawrence Berkeley National Laboratory, Berkeley, CA 94720, USA

**Abstract.** CUORE, the Cryogenic Underground Observatory for Rare Events, is an experiment searching for the neutrinoless double-beta decay of  $^{130}\text{Te}$ . The first CUORE dataset was acquired in May and June 2017 and consisted of 10.6 kg·yr of  $\text{TeO}_2$  exposure, with several days of calibration data before and after the physics dataset. We discuss here the initial performance of the CUORE detector and cryostat in this first dataset.

## 1. Introduction

Double-beta decay is a rare process in which a nucleus decays by emitting two electrons simultaneously. The ordinary form of this decay,  ${}^A_Z\text{X} \rightarrow {}^A_{Z+2}\text{X}' + 2e^- + 2\bar{\nu}_e$ , has been observed in a variety of isotopes, and generally has half-lives on the order of  $10^{19}$  to  $10^{21}$  y [1]. There is another hypothesized form of this decay, however, in which no neutrinos are released. This decay, known as neutrinoless double-beta ( $0\nu\beta\beta$ ) decay, can occur only if the neutrino is a Majorana particle; that is, if the neutrino is its own antiparticle. Observation of  $0\nu\beta\beta$  decay would be the first evidence of lepton number violation and unambiguously establish the Majorana nature of the neutrino.

Because there are no neutrinos in the final state of  $0\nu\beta\beta$  decay, the total energy of the electrons released in the decay is fixed at a specific value,  $Q_{\beta\beta}$ , which is the difference in binding energy between the initial and final nuclei. By contrast, in normal double-beta decay, the neutrinos carry away a portion of the energy, and the total energy of the electrons is a continuum from 0 to  $Q_{\beta\beta}$ . Thus, the goal of any  $0\nu\beta\beta$  decay search is to capture and record the energy of electrons released in the decay and search for an excess of events near  $Q_{\beta\beta}$ .

CUORE, the Cryogenic Underground Observatory for Rare Events, is an experiment searching for the neutrinoless double-beta decay of  $^{130}\text{Te}$  [2]. It is located deep underground, at

a depth of  $\sim$ 3600 m.w.e, at the Laboratori Nazionali del Gran Sasso in Assergi, Italy. CUORE is composed of 988  $\text{TeO}_2$  crystals, which serve as both the  $0\nu\beta\beta$  decay sources and as bolometric detectors — ultra-low temperature devices that measure the energy of incident particles via a rise in temperature. These high-resolution crystal bolometers, with a total mass of 742 kg, corresponding to 206 kg of  $^{130}\text{Te}$ , are operated at  $\sim$ 15 mK.

CUORE is a successor experiment to CUORE-0 [3] and Cuoricino [4]. The CUORE family of detectors is distinguished from other  $0\nu\beta\beta$  searches by the high natural isotopic abundance of  $^{130}\text{Te}$ , the  $Q$ -value of  $^{130}\text{Te}$  decay above the Compton edge of the dominant  $\gamma$  background (2615 keV from  $^{208}\text{Tl}$ ), and the high resolution of  $\text{TeO}_2$  bolometers ( $\sim$ 0.2% at  $Q_{\beta\beta}$ ).

## 2. CUORE Detectors and Cryostat

The 988  $\text{TeO}_2$  bolometric detectors are arranged into 19 towers, each with 13 floors of 4 crystals. The frame of each tower is copper, and the crystals are thermally coupled to the copper frame with polytetrafluoroethylene (PTFE) supports. Each crystal is instrumented with a resistive heater, which is used for stabilizing the detector gain over time, and a neutron transmutation doped germanium (NTD-Ge) thermistor [5], for measuring the crystal temperature.

Energy depositions in the  $\text{TeO}_2$  crystals are measured by continuously recording the voltage across each thermistor. Each pulse is filtered, digitized, and saved. The amplitude of each pulse is proportional to the energy deposited in the crystal, and the bolometers take  $\sim$ 5 s to recover their baseline temperature after each pulse.

CUORE is operated in a cryogen-free cryostat that cools the 742 kg of  $\text{TeO}_2$  and several tons of shielding to cryogenic temperatures. The first step is the fast cooling system, which uses liquid helium vapor to cool the cryostat to  $\sim$ 50 K. Five pulse tube cryocoolers then work to cool the detectors to  $\sim$ 4 K, and, finally, a dilution refrigerator cools the detectors to 15 mK, with a cooling power of 3  $\mu\text{W}$  of power at 10 mK. During operations, the detector temperature is stable to within  $\sim$ 0.25 mK.

Inside the CUORE cryostat is a series of copper vessels at successively colder temperatures. There is also a lead shield directly above the detectors, at 50 mK, and additional lead around the sides of the detector and below the detector, at 4 K. The lateral and bottom lead shields are composed of ancient Roman lead with especially low levels of  $^{210}\text{Pb}$ . The CUORE cryostat is suspended from a steel platform that is connected via sand-filled columns to concrete walls that are seismically isolated from the bedrock. The detectors are suspended independently from the rest of the cryostat and are further isolated from this steel platform with the use of three passive mechanical vibration isolators. During operations, a lead shield is raised around the outside of the cryostat for protection from external  $\gamma$  sources. This lead shield is also surrounded by borated polyethylene and boric acid panels, which provide protection from external neutrons.

We have employed a variety of strategies to minimize noise through vibration isolation. The pulse tube system is a primary contributor to the overall noise, as the pulse tube lines move and vibrate continuously when in operation. We mitigate this noise in a variety of ways. Cold mechanical decouplers above the 40 K and 4 K plates isolate the colder cryostat stages from the vibrations that the pulse tube lines induce on the top (room-temperature) cryostat plate. We also use remote motor heads that are suspended independently from the cryostat and from the detectors. Finally, we have implemented active phase cancellation between the 5 pulse tubes, following a scan to select the most desirable relative phases.

## 3. Data acquisition

The first CUORE dataset was acquired in May and June 2017. The dataset began and ended with approximately 3 days of calibration with  $^{232}\text{Th}$  sources. Of the 988 total bolometers, 984 (99.6%) are operational; this first analysis is performed with the best-performing 889 (90%) bolometers. We acquired 38.1 kg·yr of exposure with these 889 channels, corresponding to

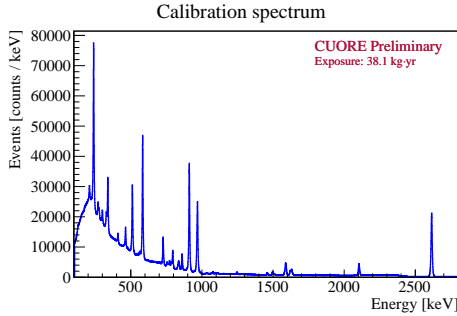


Figure 1: Calibration spectrum from the first CUORE dataset.

10.6 kg·yr of  $^{130}\text{Te}$  exposure. In total, 65% of the run time in this dataset was devoted to physics data taking, with 22% devoted to calibration and the rest to test and other operations.

Calibration is performed by a semi-automated system that lowers warm  $^{232}\text{Th}$  calibration sources into the cryostat and cools them to base temperature monthly [6]. The use of internal sources is necessary due to the tightly-packed array of detector towers and the presence of shielding inside the cryostat, both of which limit our ability to effectively use calibration sources external to the cryostat. We use several lines from the  $^{232}\text{Th}$  decay chain to calibrate the detector, including the 239 keV line from  $^{212}\text{Pb}$ ; 338 keV, 911 keV, and 969 keV lines from  $^{228}\text{Ac}$ ; and 583 keV and 2615 keV lines from  $^{208}\text{Tl}$  (see Figure 1).

We acquire data continuously from each of the 984 operational detectors at a sampling rate of 1 kHz. Data is acquired in runs of approximately 1 day and grouped into datasets of approximately 1 month. Each dataset begins and ends with a calibration to ensure that the detector response has not changed over the course of the month. At the end of each dataset, we compute an average pulse shape and average noise power spectrum and use this to filter the software-triggered 5-second waveforms. We then compute the amplitude of each filtered pulse by looking for the first local maximum in the signal after the trigger and extrapolating between the points on either side of the maximum.

Using the silicon heaters attached to the crystals, we periodically inject fixed amounts of energy into the crystals over the course of the dataset. We use these pulses to stabilize the detector gain over the dataset. We then search for the known energy of peaks in the calibration spectrum to get a mapping from this stabilized amplitude to a true energy, which is stable on time scales of at least 1 month.

In order to select  $0\nu\beta\beta$  decay candidate events, we apply a variety of cuts to the data. Several pulse-shape parameters are measured, and we set limits on a combination of the baseline slope, pulse rise time and shape, and decay time and shape. Any  $0\nu\beta\beta$  decay events would be entirely contained in 1 crystal 88% of the time, so we also exclude events that happen in coincidence with (within 5 ms of) events in other bolometers.

#### 4. Resolution and energy reconstruction

The resolution and response function of each detector is calculated from a fit to the  $^{208}\text{Tl}$  2615 keV line in calibration data. We estimate the resolution of the physics data by comparing the resolution of the 2615 keV line in physics data to that of calibration data. We do not have enough statistics to do an independent fit to the 2615 keV line in physics data in each channel, so we use the line shape and resolutions in calibration data. Because the 2615 keV line is close to  $Q_{\beta\beta} = 2528$  keV [7], we take this to be the approximate resolution of a potential  $0\nu\beta\beta$  signal.

In all, we find that the harmonic mean of our channel resolutions in calibration data is 10.6 keV at 2615 keV (see Figure 2), and the resolution of the physics data is 74% of the calibration data resolution. Thus, the resolution of our physics data is estimated to be

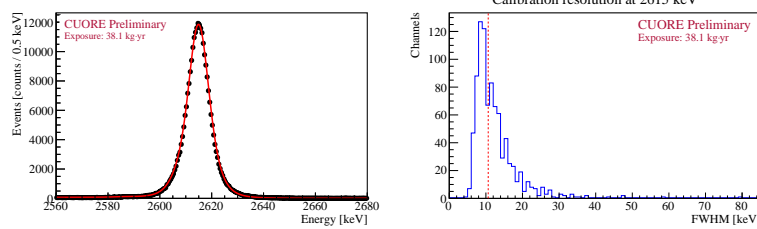


Figure 2: Left: Simultaneous fit to the 2615 keV calibration line in all channels. Right: Distribution of calibration resolutions at the 2615 keV line for these channels.

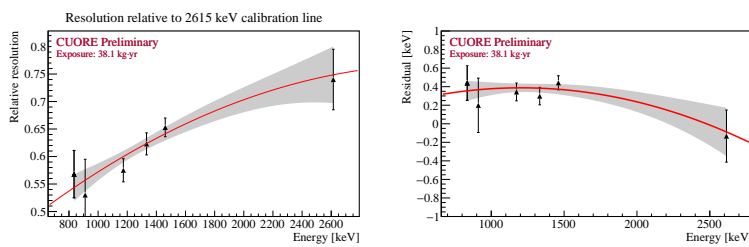


Figure 3: Left: Resolution of lines in the physics spectrum relative to that of the 2615 keV calibration line. Right: Difference between reconstructed energy and nominal energy for peaks in the physics spectrum.

$(7.9 \pm 0.6)$  keV at 2615 keV.

We also use the visible peaks in the physics spectrum to estimate the resolution of lines in the physics spectrum at different energies and the energy bias of our data processing (see Figure 3). We find that our energy reconstruction is accurate to within 0.5 keV, which we treat as a systematic uncertainty in our  $0\nu\beta\beta$  decay fit.

## 5. Future prospects

CUORE plans to accumulate 5 years of live time over the course of the experiment. Our expected 5-year sensitivity is  $T_{1/2}^{0\nu} > 9 \times 10^{25}$  yr [8]. In the framework of  $0\nu\beta\beta$  decay mediated by light Majorana neutrino exchange, this corresponds to a limit on the effective Majorana neutrino mass of  $m_{\beta\beta} > 60 - 160$  meV, depending on the nuclear matrix elements used.

## 6. Acknowledgments

The CUORE Collaboration thanks the directors and staff of the Laboratori Nazionali del Gran Sasso and the technical staff of our laboratories. This work was supported by the Istituto Nazionale di Fisica Nucleare (INFN); the National Science Foundation; the Alfred P. Sloan Foundation; the University of Wisconsin Foundation; and Yale University. This material is also based upon work supported by the US Department of Energy (DOE) Office of Science; and by the DOE Office of Science, Office of Nuclear Physics. This research used resources of the National Energy Research Scientific Computing Center (NERSC).

## References

- [1] Alduino C *et al.* (CUORE Collaboration) 2017 *Eur. Phys. J. C* **77** 13
- [2] Artusa D R *et al.* (CUORE Collaboration) 2015 *Adv. High Energy Phys.* **2015** 1–13
- [3] Alfonso K *et al.* (CUORE Collaboration) 2015 *Phys. Rev. Lett.* **115** 102502
- [4] Andreotti E *et al.* (Cuoricino Collaboration) 2011 *Astropart. Phys.* **34** 822–831
- [5] Haller E E, Palaio N P, Rodder M, Hansen W L and Kreysa E 1984 *Neutron Transmutation Doping of Semiconductor Materials* (Boston, MA: Springer US) pp 21–36 ISBN 978-1-4612-9675-1
- [6] Cushman J S *et al.* 2017 *Nucl. Instr. Meth. A* **844** 32–44
- [7] Redshaw M, Mount B, Myers E and Avignone F 2009 *Phys. Rev. Lett.* **102** 212502
- [8] Alduino C *et al.* (CUORE Collaboration) 2017 *Eur. Phys. J. C* **77** 532